


Article

Quantitative Estimation of COD Values from an Array of Metal Nanoparticle Modified Electrodes and Artificial Neural Networks †

Qing Wang, Xavier Cetó and Manel del Valle * 

Sensors and Biosensors Group, Department of Chemistry, Universitat Autònoma de Barcelona, Bellaterra, 08193 Barcelona, Spain

* Correspondence: manel.delvalle@uab.cat

† This paper is an extended version of the conference paper: Wang, Q.; del Valle, M. Determination of Chemical Oxygen Demand (COD) Using Nanoparticle-Modified Voltammetric Sensors and Electronic Tongue Principles. In Proceedings of the 1st International Electronic Conference on Chemical Sensors and Analytical Chemistry (CSAC2021), 1–15 July 2021.

Abstract: Water quality monitoring has become critical in modern societies in multiple areas and at different stages. In this regard, chemical oxygen demand (COD) has become a key index in water testing, as it readily allows the determination of its overall quality and the presence of organic contaminants. However, conventional COD determination presents several drawbacks in view of the use of toxic reagents and possible interferences. The electrochemical determination of COD can be an alternative with many advantages, especially if using an array of sensors. Herein, the use of an electronic tongue (ET) for the estimation of COD was explored. The proposed ET was formed by an array of five voltammetric electrodes modified with different metal nanoparticles. An artificial neural network (ANN) model was built based on the responses of the array towards glucose and glycine as standards. This model was then used with real and spiked water samples, and the results compared to the electrochemical calibration and the commercial COD colorimetric methods. While the COD values of the real samples were low and outside the range of the ANN model, a satisfactory prediction for the spiked samples was achieved, showing a good agreement with the reference colorimetric method, that was better than the performance of the conventional electrochemical calibration method.

Keywords: chemical oxygen demand; wastewater; metal nanoparticles; voltammetric sensors; artificial neural networks; electronic tongue



Citation: Wang, Q.; Cetó, X.; Valle, M.d. Quantitative Estimation of COD Values from an Array of Metal Nanoparticle Modified Electrodes and Artificial Neural Networks.

Chemosensors **2022**, *10*, 504. <https://doi.org/10.3390/chemosensors10120504>

Academic Editor: Nicole Jaffrezic-Renault

Received: 28 October 2022

Accepted: 23 November 2022

Published: 28 November 2022

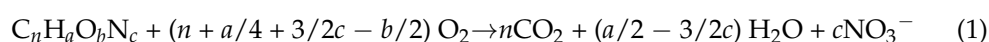
Publisher's Note: MDPI stays neutral with regard to jurisdictional claims in published maps and institutional affiliations.



Copyright: © 2022 by the authors. Licensee MDPI, Basel, Switzerland. This article is an open access article distributed under the terms and conditions of the Creative Commons Attribution (CC BY) license (<https://creativecommons.org/licenses/by/4.0/>).

1. Introduction

Chemical oxygen demand (COD) is a widely used parameter in the evaluation of the total organic compounds present in water, especially in wastewater. The value of COD is expressed as the amount of molecular oxygen (in milligrams of O₂ per liter) required to oxidize all organic compounds to carbon dioxide and water according to Equation (1). The amino nitrogen will be converted to nitrate in the presence of an oxidizing agent [1–6].



To ensure that all organic matter is fully oxidized according to the above reaction, the use of a strong oxidizer under acidic conditions and reflux temperature is normally used; being potassium dichromate the one used in the traditional standard procedure of COD determination. However, it involves hexavalent chromium as reagent, which in addition to being poisonous, is also not environment-friendly [7]. As an alternative, potassium permanganate can also be employed, as it is less toxic than potassium dichromate. Nevertheless, since it is a weaker oxidant, it is not able to oxidize all the organic compounds in water [8]. Moreover, the traditional COD test consists of several steps and complicated

operations, which are very time-consuming and troublesome [9]. To avoid the difficulties derived from the traditional measurement, substantial efforts have been directed towards the development of more friendly methods. Because of their good sensitivity, low cost and effortless operation, electrochemical methods have attracted much attention as an alternative for the determination of COD [10–14].

Electrochemical methods offer a rapid and simple estimation of COD, from the potential equivalence of biochemical and electrochemical oxidation. Furthermore, they do not require the use of those toxic and expensive reagents used in the traditional method. Instead, calibration curves are obtained based on the reaction of organic compounds oxidized by radicals generated electrochemically on the electrode [15]. Because of the ease of operation, they offer the possibility of implementing online COD determination systems. For example, Duan and coworkers developed a compact analytical platform that integrates an electrochemical deposited copper nanoparticle-based (Cu NPs) carbon/silicon dioxide(C/SiO₂) thin-film electrochemical sensor, which achieved on-line monitoring of COD in urban wastewater [16].

Over the last few years, many materials have been reported as electrocatalysts in the amperometric determination of COD, essentially with use of metal nanoparticles (NPs) [8,9,12–15], or oxide films [16–20]. For the calibration of the sensors, most often a single standard organic compound is used to simulate the wastewater components (e.g., glucose or potassium hydrogen phthalate), and the calibration curves of current intensity vs. the COD values are built, based on the concentration of the standard compound taking the Equation (1) mentioned above. Such a method has shown a satisfactory performance in the COD determination towards wastewater samples of simple composition [9,14,15,21–23]. However, the accuracy of this method is quite limited in the analysis of wastewater that consists of mixtures of organic components, each with different reactivity. In light of this consideration, a more powerful and flexible technique for nonlinear regression attracted us, namely, artificial neural networks (ANNs) [24,25]. ANNs are bio-inspired mathematical models and have been employed in the field of chemometrics for qualitative and quantitative multivariate analysis [26–29]. What makes them different from the classic linear regression methods for data treatment is their capacity to find non-linear relationships between different variables in the data, and this is also their most outstanding advantage [30].

As a case of principle, and to hypothesize the resolution of complex mixtures composed of several different organic compounds with different oxidation kinetics, we have designed an experiment that employs glucose and glycine as the organic standard substances, several voltammetric sensors as the mean to generate sufficient information [31], and an ANN response model to estimate the COD values. A total of five sensors were used, four of which were made of carbon modified with different metal NPs, plus an additional CuO sensor made of NPs electrogenerated over a Cu block. The system was trained to quantitatively predict the organic load (COD value) of mixtures of two compounds—in this case, glucose and glycine. The generated model has been validated with a separate set of test samples, consisting of other mixtures of the same two compounds. In summary, this paper presents a new method for predicting organic load properties in wastewaters, based on cyclic voltammograms and ANNs.

2. Experimental

2.1. Chemicals and Reagents

The reagents used in this work were of analytical reagent grade and were used as received without any further purification. All solutions were prepared using Milli-Q water purified by a Milli-Q system (Millipore, Billerica, MA, USA). The following metallic NPs were used as modifiers during the fabrication of the electrodes: copper (Cu NPs, 40~60 nm) and copper (II) oxide (CuO NPs, <50 nm) which were purchased from Sigma-Aldrich (St. Louis, MO, USA), and nickel copper alloy (Ni Cu NPs, <80 nm) purchased from Nanografi Nano technology (Ankara, Turkey). Alumina powder (γ type), which was used for polishing the surface of the copper block, was purchased from CH Instruments (Austin,

TX, USA). Glycine, sodium hydroxide and sodium chloride were purchased from Sigma-Aldrich (St. Louis, MO, USA). Glucose was obtained from Panreac (Barcelona, Spain). Graphite powder (<50 μm) and the epoxy resin kit, both used for the construction of the electrodes, were purchased from BDH (BDH Laboratory supplies, Poole, UK) and Resineco Green Composites (Barcelona, Spain), respectively.

2.2. Apparatus

Voltammetric measurements were conducted in a PGSTAT 30 Autolab potentiostat (EcoChemie, Utrecht, The Netherlands) with GPES 4.7 version software (EcoChemie). Electrochemical measurements were carried out in a conventional three-electrode cell configuration composed of the 5 fabricated electrodes as the working electrodes; and a metallic platinum electrode (Crison 5261, Barcelona, Spain) and a Ag/AgCl electrode, as the auxiliary and reference electrodes, respectively. In the manner described below, a cyclic voltammogram was recorded for each of the electrodes by sweeping the potential between -0.1 V and $+0.8$ V, with a step potential of 0.01 V and a scan rate of 100 mV/s.

For the morphological characterization of the electrodes, images were collected using scanning electron microscope (SEM) EVO[®]MA10 from Zeiss (Oberkochen, Germany).

The commercial cuvettes for the sealed tube colorimetric COD determination were bought from HACH (HACH LANGE GMBH, Dusseldorf, Germany). Measurements were completed with the DR3900 laboratory spectrophotometer (HACH).

2.3. Electrode Fabrication

Two distinct kinds of electrodes were used in this work: a surfaced-modified copper block electrode and 4 bulk-modified graphite-epoxy composite (GEC) electrodes. The electrodes were fabricated according to the previously reported procedures [14,21]. Briefly, in the case of the copper electrode, the electrode surface was first polished using alumina powder, and cleaned with Milli-Q water; copper (II) oxide (CuO) nanoparticles were then deposited on its surface by cycling the potential between -0.1 to $+0.8$ V in a 0.05 M NaOH solution for 50 cycles; this electrode will be referred as CuO/Cu in this report. As for the GEC electrodes, these were prepared by mixing 54% of graphite, 41% of the epoxy resin and 5% of the modifier. Next, this mixture was inserted into a PVC tube, where a connector had previously been introduced, and allowed to harden for 2 days at 40 °C. In this manner, 4 different electrodes were prepared employing Cu NPs, CuO NPs, Ni Cu NPs and Ni NPs as the modifiers, which will be used to refer to the respective electrodes from now.

2.4. Data Analysis

Collected voltammograms were first analyzed employing the GPES Multichannel 4.7 software package (EcoChemie, Utrecht, The Netherlands) to accomplish the analytical characterization of the different sensors' response. In this manner, calibration plots were built from which the usual parameters such as the sensitivity, linearity, limit of detection (LOD), repeatability, etc., were assessed.

For the estimation of the COD index, a chemometric model was built using ANNs as the modeling tool. Briefly, recorded voltammograms were unfolded, and causal index (CI) analysis was used to reduce the dimensionality of the recorded voltammograms [32]. Next, the ANN topology was optimized to find the best configuration that optimizes its performance. This data processing was done in Matlab 7.1 (MathWorks, Natick, MA, USA) by specific routines developed by the authors using the Neural Network toolbox.

2.5. Samples under Study

For the characterization of the electrodes' response, glucose and glycine stock solutions were prepared in 0.05 M NaOH, from which solutions of increasing concentration of each compound were prepared and measured with the different sensors.

For the estimation of COD values, a set of samples consisting of mixtures of glucose and glycine were also prepared, with concentrations ranging from 0.25 mM to 4.00 mM

of glucose and 0.40 mM to 6.25 mM of glycine, to simulate a real case in which different compounds with different reactivity are present. To obtain the ANN response model, a training set was used (16 samples); a further testing set (10 samples) was used to assess the model's performance. The concentration of the former was based on a tilted factorial design with 2 factors and 4 levels (2^4), while the latter had the concentrations randomly distributed along the experimental domain defined by the former.

Lastly, 5 real water samples were collected from different rivers and streams throughout Catalonia (Spain). The first sample (R1) was from a stream alongside a farm in Ripollet. Two more samples (R2 and R3) were from the two tributary streams of the river Llobregat in Gavà, flowing alongside the farms. R4 was from the river across Sant Boi de Llobregat. Finally, R5 was from a river near to a farm in Lleida. Additionally, these 5 samples were spiked with different concentrations of glucose and/or glycine (S1–S5) to assess the recovery values from the values predicted by the ANN.

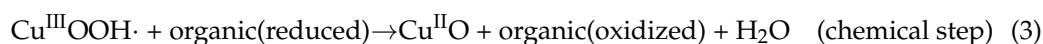
These real samples were analyzed both electrochemically with the proposed sensor array as well as with the colorimetric COD reference method. For the electrochemical measurements, samples were mixed with 0.1 M NaOH (1:1, *v/v*) to have the same supporting electrolyte. The voltammetric responses of the electrode array towards these samples were recorded in a cycled potential range from 0 to 1.0 V with a scan rate of 50 mV/s.

The reference COD determinations of these samples were also conducted using dichromate reagent with the sealed tube colorimetric method. After placing the sample in the tube with pre-dosed reagents, these were heated for 2 h at 148 °C. Cuvettes of two different measuring ranges were used, for 5~60 mg/L O₂ and 100~2000 mg/L O₂, respectively. COD values were obtained after colorimetric reading, with factory-defined calibration curves.

3. Results and Discussion

3.1. Preparation of the CuO/Cu Electrode

Copper has been reported as a powerful electrocatalyst for the oxidation of carbohydrates and amino acids, which added to its good electrical conductivity [4], makes it an interesting material for the electrochemical estimation of COD [21–23]. Moreover, alkaline media have also been reported to improve the performance of copper-based electrodes for the oxidation of organic compounds [23]. Their electrocatalytic behavior lies in the action of radicals generated on the sensor surface [4]. As reported in previous studies [21–23], the performance of this kind of electrode can be affected by the hydroxide concentration and the pre-formation of a specific layer of CuO. Furthermore, Cu(III) species also take part in the reaction as an important electron transfer mediator [33]. The electrocatalytic behavior of CuO involved in the oxidation of organic compounds was proposed as follows by Silva et al. [21]:



For this reason, in this work, the use of a copper disk electrode modified with CuO NPs (CuO/Cu), which was also incorporated in the sensor array, was the first choice. CuO NPs were formed and deposited electrochemically as described in Section 2.3. As illustrated in Figure 1, the deposition showed three differentiated stages: The initial step was the formation of a first layer of copper (I) oxide (Cu₂O), corresponding to the anodic peak at around −0.30 V (vs. Ag/AgCl) observed in Figure 1a. The decrease of the current intensity at this potential occurred as the copper (I) transformed to Cu (II) after losing electrons, as indicated with down arrows in Figure 1a,b. The formation of a second mixed layer that evolves during preparation of the electrode was indicated by a broader anodic peak appearing at −0.10 V, as the right arrow indicates in Figure 1a,b. Finally, once stabilized, the broad anodic peak at around −0.05 V (vs. Ag/AgCl) increased as indicated in Figure 1c,

suggesting the formation of a durable layer of a mixture of copper (II) oxide and copper (II) hydroxide. In all cases, the two cathodic peaks observed at -0.60 V and -0.90 V (vs. Ag/AgCl) correspond to the reduction of Cu(II)/Cu(I) and Cu(I)/Cu(0), respectively.

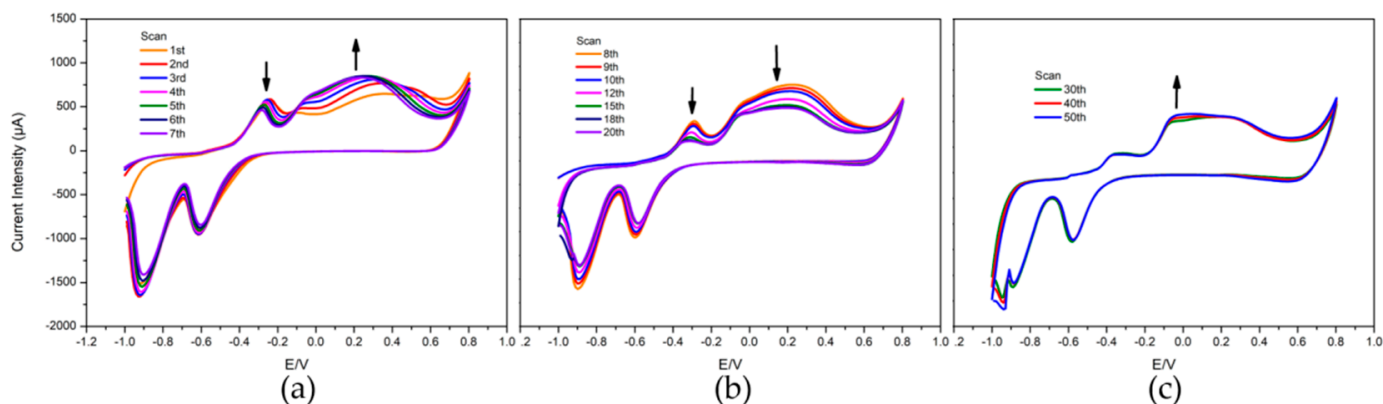


Figure 1. Cyclic voltammograms corresponding to the electrochemical formation of CuO on the surface of the copper, that alters the electrode surface in three distinct stages (a–c), observed during its preparation. Electrochemical measurements were performed at 100 mV/s in 0.05 M NaOH for 50 cycles.

During the electrochemical deposition, the color of the electrode surface changed from the initial glossy yellow of copper to dark brown, characteristic of copper oxide. To further confirm the surface modification, SEM images before and after the modification of the electrode were taken, as shown in Figure 2. As the CuO NPs formed, it spread over the electrode, which made the surface look rougher. This rougher surface is helpful to increase the electro-catalytic oxidation activity. The SEM images of the other four NPs-modified electrodes are also shown in Figure 2c–f.

3.2. Voltammetric Response of the Electrodes

After the fabrication of the electrodes, the next step was the evaluation of their voltammetric responses towards glucose and glycine. These were selected as model compounds prior to proceeding with the determination of the total COD. For this, 0.05 M NaOH was chosen as the supporting electrolyte, which provided the required mild alkaline condition [22].

The corresponding measurements were conducted with standard solutions of glucose and glycine (with COD value 400 mg/L O₂) employing the prepared sensor array. As shown in Figure 3, glucose and glycine can be oxidized at the surface of all the considered electrodes, but with the oxidation occurring at different potentials for each of them. For example, the oxidation of glucose and glycine on the CuO/Cu electrode occurs at 0.5–0.6 V and 0.7–0.8 V, respectively, while in the case of the Ni NPs modified GEC electrode, oxidation of both occurred at around 0.6–0.7 V. Furthermore, it should be noted that the associated current intensities for the CuO/Cu electrode are much higher than those of the other electrodes, possibly attributable to the generated NPs on the electrode surface. The fact that the different electrodes each show different behavior towards the different analytes is highly desirable when developing ET applications. To complete the characterization, voltammetric responses of the different electrodes in the array were recorded against increasing theoretical COD values, for glucose and for glycine, respectively. The responses of the electrodes towards glucose are shown in Figure 4, with a COD range from 0 to 1000 mg/L O₂, while those towards glycine are shown in Figure 5, with a COD range from 0 to 400 mg/L O₂. Table 1 summarizes the fitted calibration lines obtained for the CuO/Cu electrode.

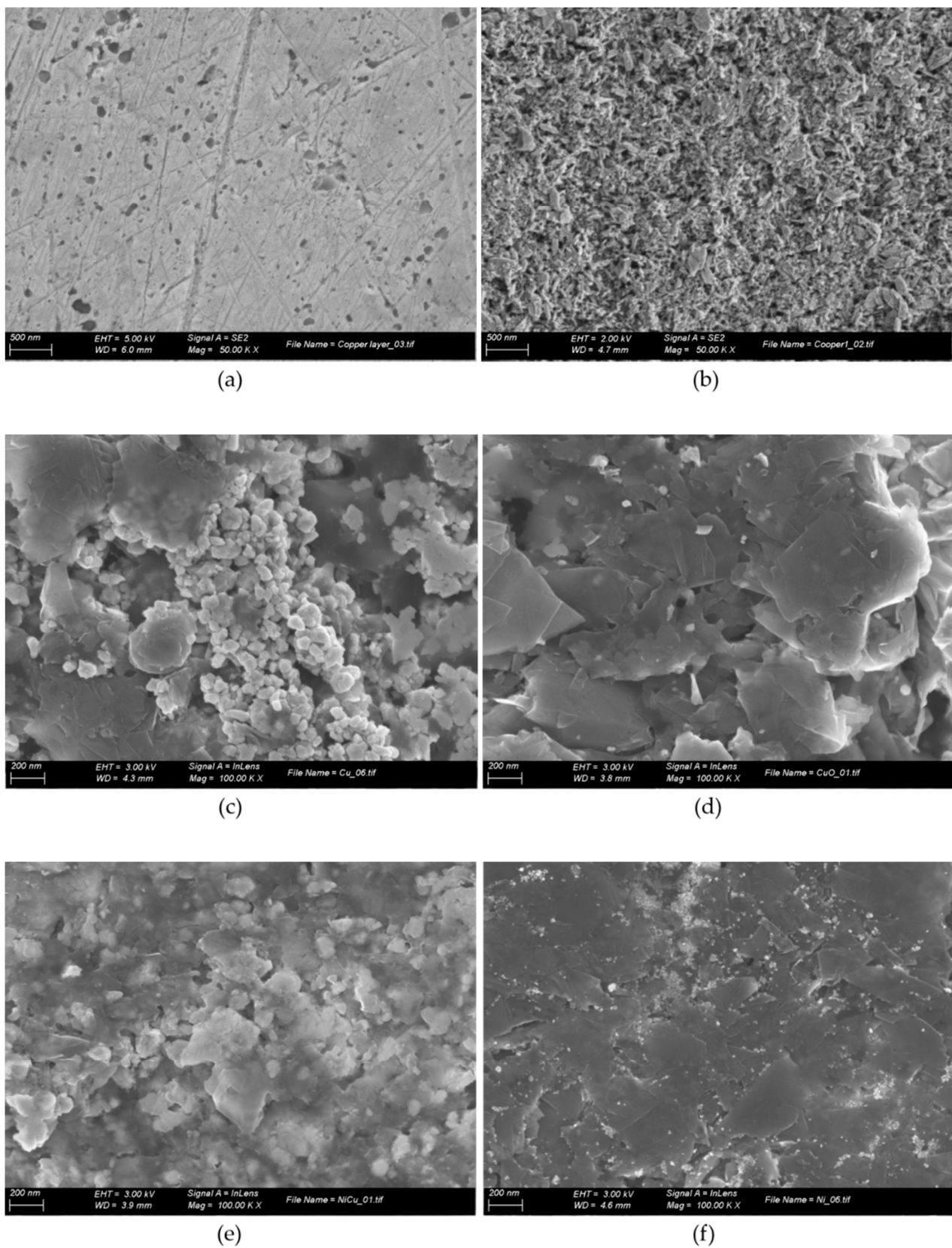


Figure 2. Scanning electron microscopy (SEM) characterization of (a) bare polished Cu block; (b) electrodeposited electrode CuO/Cu and the four modified GECs with: (c) Cu NPs, (d) CuO NPs, (e) Ni Cu NPs, (f) Ni NPs.

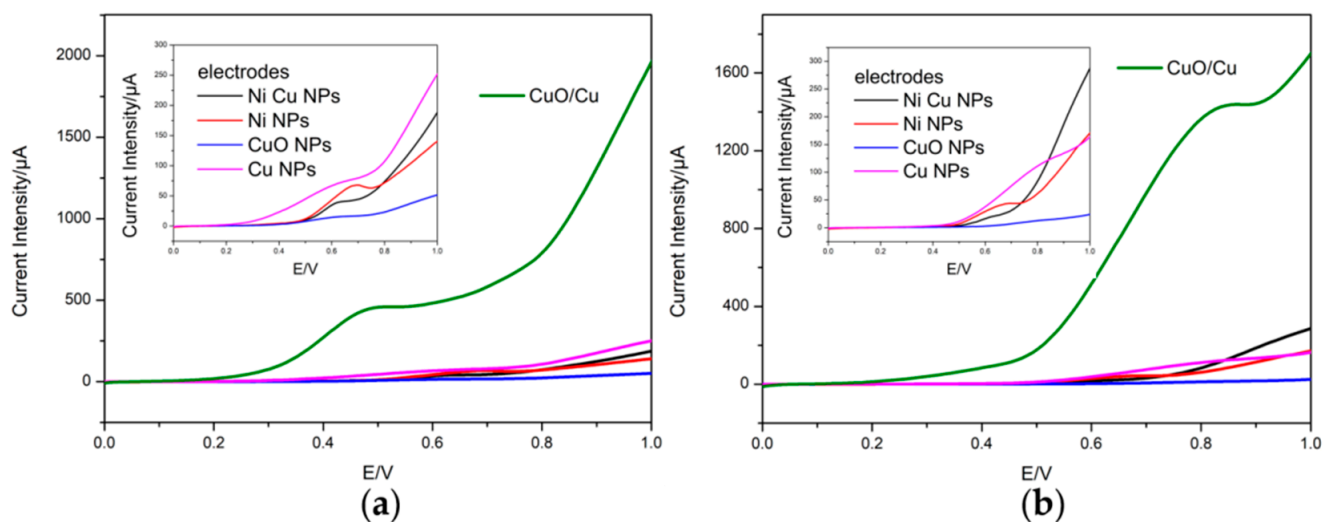


Figure 3. Voltammetric responses of the different electrodes obtained for (a) glucose and (b) glycine solutions, with a theoretical COD value of 400 mg/L O₂ in 0.05 M NaOH electrolyte with a scan rate of 50 mV/s.

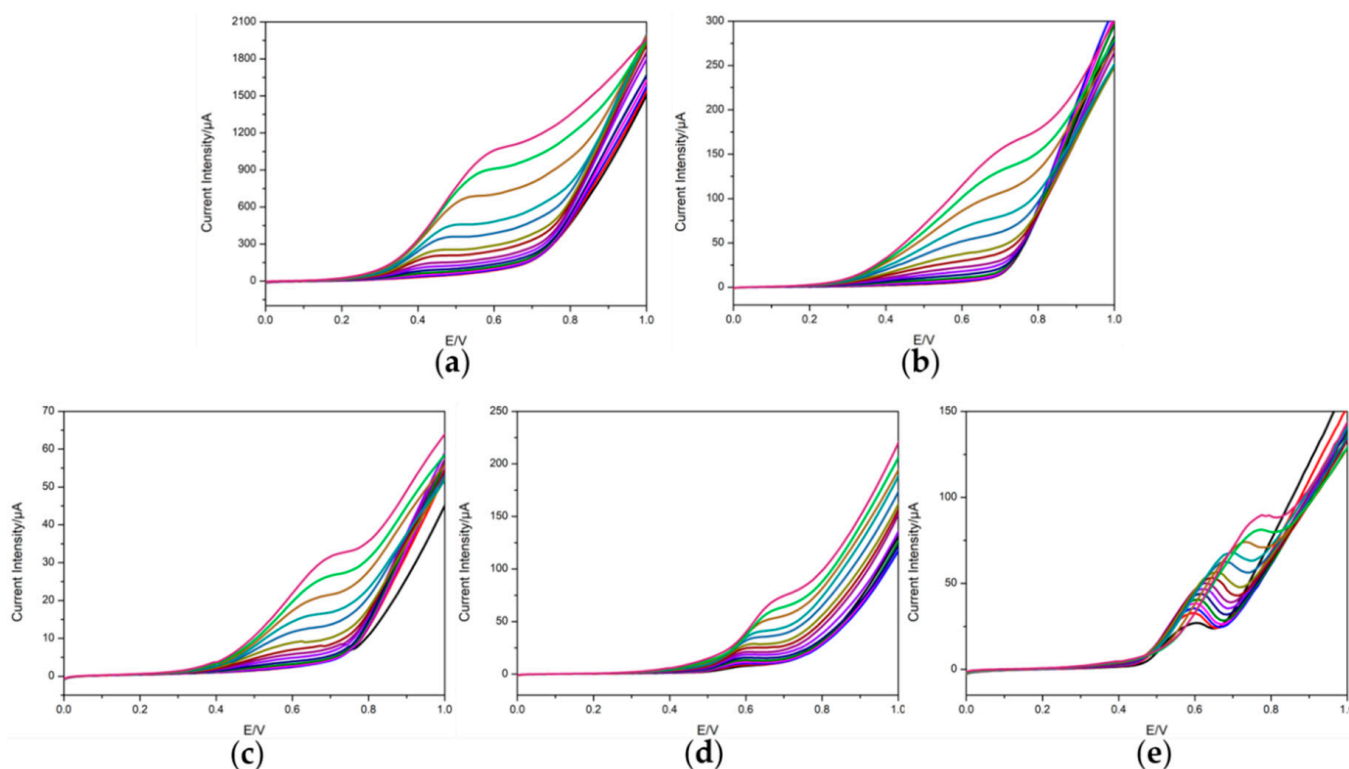


Figure 4. Voltammetric responses of the different electrodes—(a) CuO/Cu, (b) Cu NPs, (c) CuO NPs, (d) Ni Cu NPs and (e) Ni NPs—to glucose solutions of increasing theoretical COD values from 0 to 1015 mg/L O₂ in 0.05 M NaOH with a scan rate of 50 mV/s.

Table 1. Calibration lines of the electrode CuO/Cu towards the two organic compounds, glucose and glycine, at the fixed potentials of +0.6 and +0.7 V, respectively.

| Compound | Equation | Linear Range | Limit of Detection |
|----------|--------------------------------------|----------------------------|--------------------------|
| Glucose | $y = 1.0281x + 85.90, R^2 = 0.9996$ | 30~800 mg/L O ₂ | 15.7 mg/L O ₂ |
| Glycine | $y = 3.3315x + 167.19, R^2 = 0.9991$ | 10~180 mg/L O ₂ | 4.6 mg/L O ₂ |

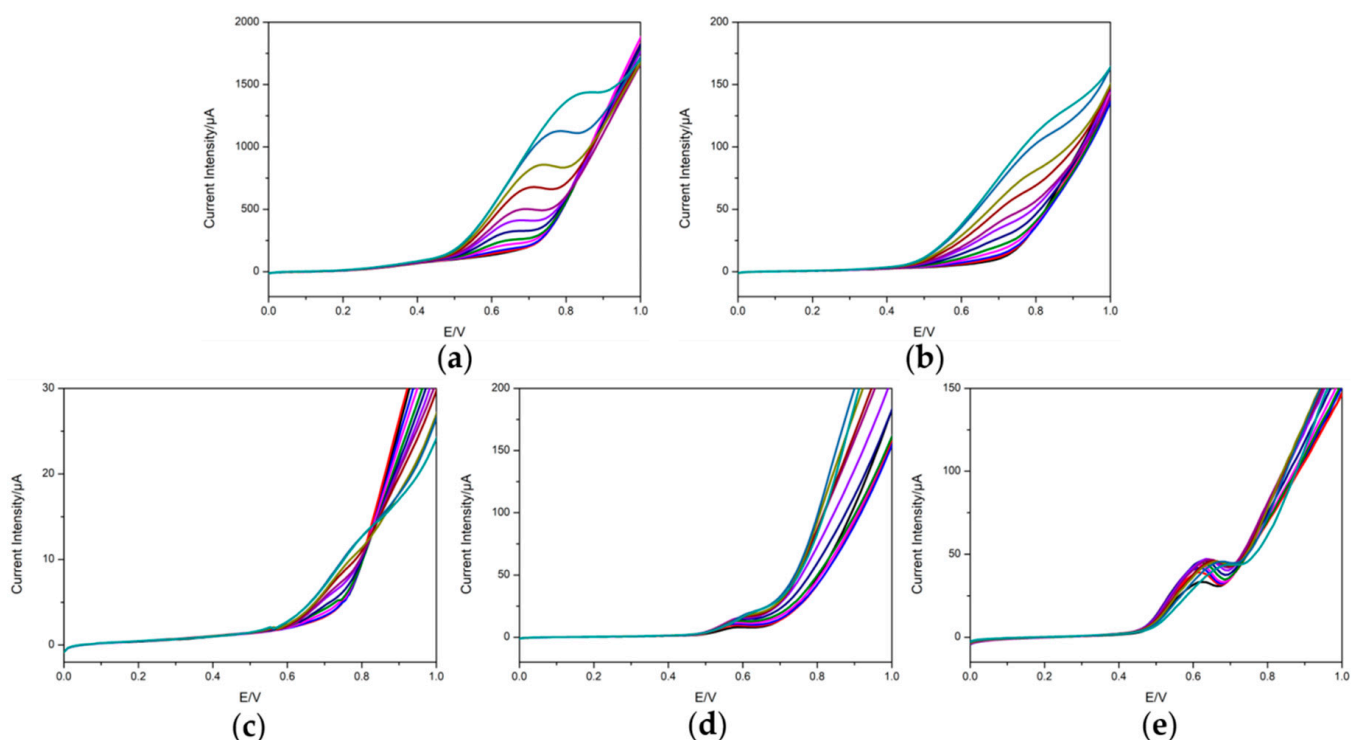


Figure 5. Voltammetric responses of the different electrodes—(a) CuO/Cu, (b) Cu NPs, (c) CuO NPs, (d) Ni Cu NPs and (e) Ni NPs—to glycine solutions of increasing theoretical COD values from 0 to 400 mg/L O₂ in 0.05 M NaOH with a scan rate of 50 mV/s.

3.3. Repeatability

To complete the analytical characterization of the sensors' response, the next step was studying its repeatability. Ensuring that repetitive measurements can be obtained when a new sensing device is developed is always important, but this is especially critical when developing ET applications, as the sensors need to withstand the larger number of measurements, as required to build the chemometric model in comparison to a univariate calibration model.

To this aim, the voltammetric responses of the five electrodes towards a mixed solution of glucose and glycine (equivalent to a COD value of 300 mg/L O₂) were evaluated for 10 consecutive measurements, during which a blank (NaOH 0.05M) was also measured in between. The corresponding measurements are shown in Figure 6, where the overlapping between the different curves clearly evidences the good response of the sensors. Furthermore, the relative standard deviation (RSD) was calculated over 10 measurements based on the current intensity at 0.6 V and 0.7 V. As can be seen in Table 2, the percentage RSD change was found to be smaller than 5% in all the cases, thus indicating the good repeatability of the electrodes' response.

Table 2. Repeatability as the percentage of the RSD (RSD%) over 10 consecutive measurement cycles of blank/standard for each of the electrodes.

| Sensor | RSD% ¹ | RSD% ² |
|-----------|-------------------|-------------------|
| CuO/Cu | 2.91% | 2.64% |
| Cu NPs | 3.60% | 2.21% |
| CuO NPs | 3.95% | 2.69% |
| Ni Cu NPs | 0.69% | 2.88% |
| Ni NPs | 3.19% | 2.80% |

^{1,2} Calculated based on the current intensity at E = 0.6 V and E = 0.7 V, respectively.

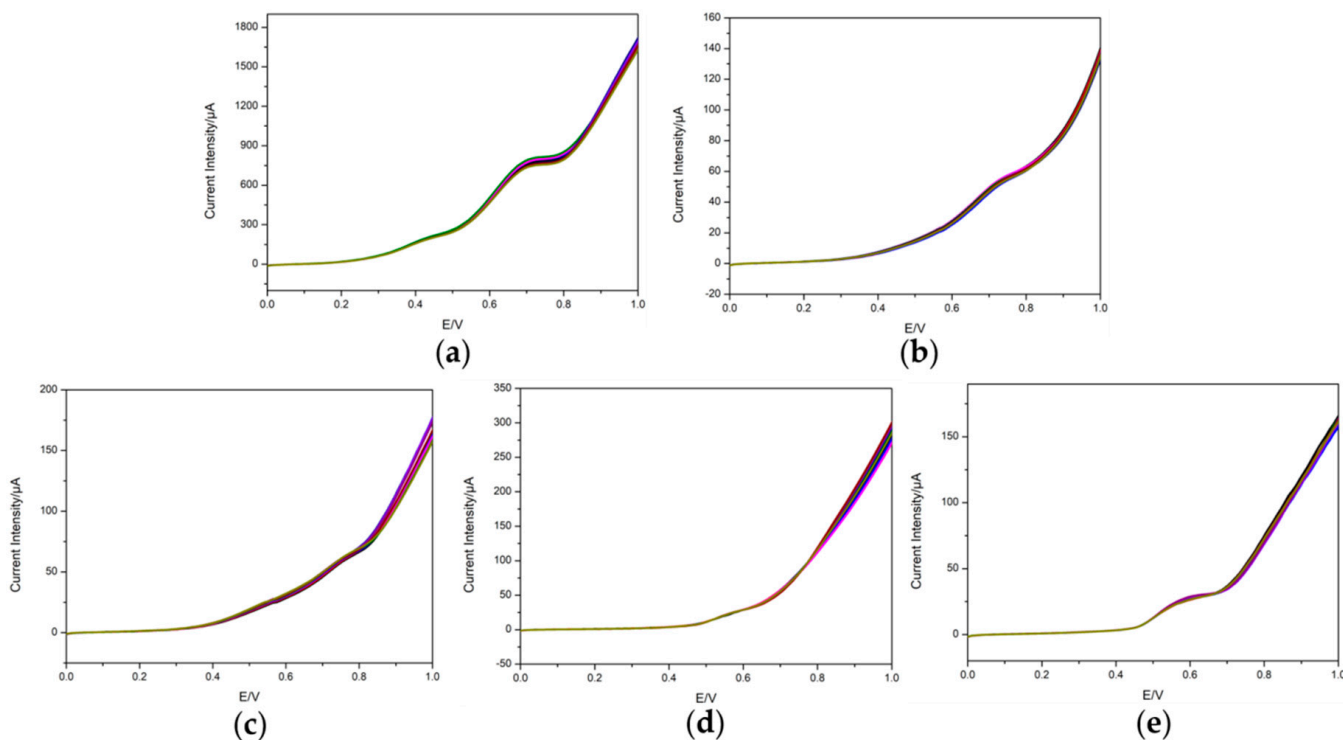
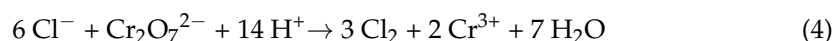


Figure 6. Ten repeated scans of cyclic voltammetric responses of the different electrodes—(a) CuO/Cu, (b) Cu NPs, (c) CuO NPs, (d) Ni Cu NPs and (e) Ni NPs—to the mixture of glucose and glycine in 0.05 M NaOH electrolyte with a scan rate of 50 mV/s.

3.4. Interference of Chloride Ions

Unlike in the conventional COD test, the presence of halides does present a problem when carrying out the estimation of COD electrochemically [3,6,34]. This problem features in the conventional test in that, on the one hand, halides can react with dichromate to produce the elemental form of the halogen and chromium(III), as shown in Equation (4), leading to an overestimation of the COD value. On the other hand, to ensure the efficient oxidation of straight-chain aliphatic compounds, silver sulfate is added as a catalyst which, in the presence of chloride or bromide, will lead to the precipitation of the corresponding silver salt, thus deactivating the catalyst and leading to an underestimation of the actual COD value. With the intention of overcoming such interference, mercuric sulfate is used to complex chloride before the reflux.



Therefore, because of its common existence, chloride ion is one of the major factors affecting COD detection. In this research, the interference of chloride ion to the voltammetric response was investigated towards increasing concentrations of NaCl added into a mixture of glucose and glycine (equivalent to a COD value of 300 mg/L O₂). From Figure 7, the voltammetric signals did not show any influence in the presence of Cl[−], as could be expected. Furthermore, the RSD% values were also calculated as carried out in Section 3.4, where the low values again indicate the good behavior of the system (Table 3).

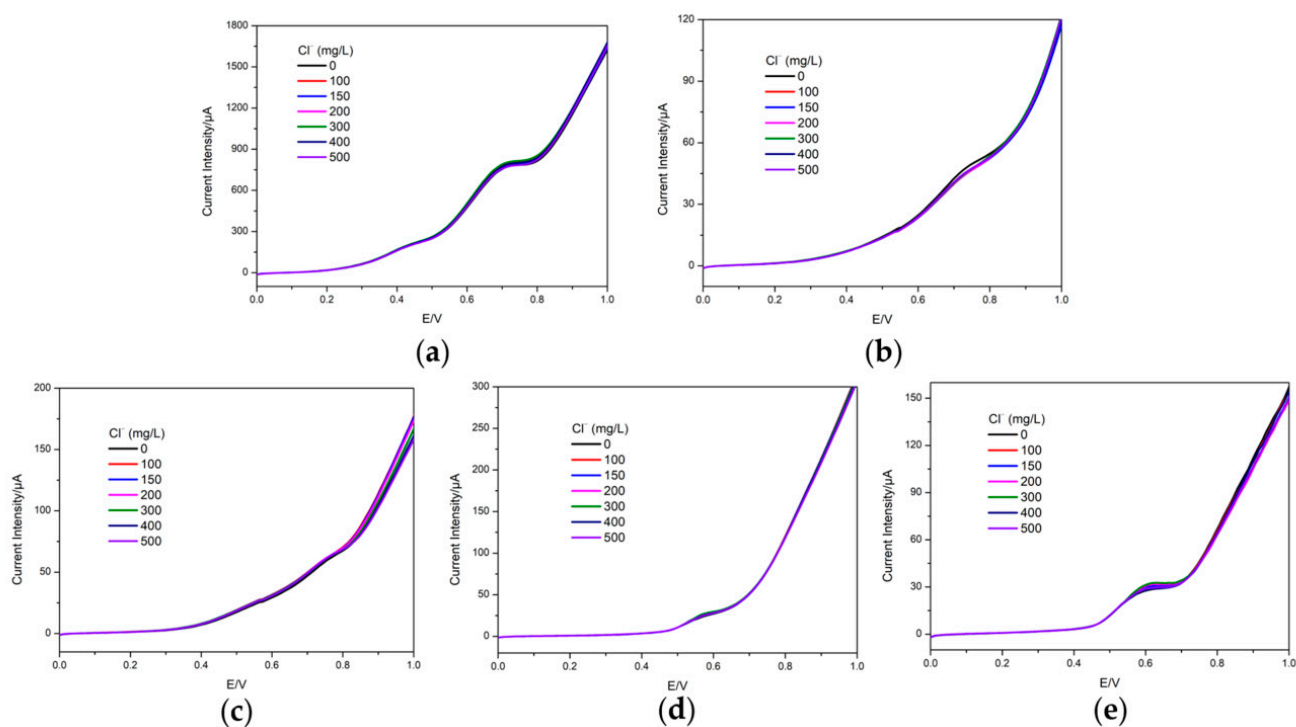


Figure 7. Cyclic voltammetric responses of the different electrodes—(a) CuO/Cu, (b) Cu NPs, (c) CuO NPs, (d) Ni Cu NPs and (e) Ni NPs—to the mixture of glucose and glycine in 0.05 M NaOH electrolyte with an increasing concentration of Cl^- . Scan rate: 50 mV/s.

Table 3. Change in the variation of the voltammetric signal due to the presence of Cl^- as the percentage of the RSD (RSD%) for each of the electrodes.

| Sensor | RSD% ¹ | RSD% ² |
|-----------|-------------------|-------------------|
| CuO/Cu | 1.82% | 1.43% |
| Cu NPs | 1.63% | 2.22% |
| CuO NPs | 2.84% | 1.97% |
| Ni Cu NPs | 2.94% | 1.00% |
| Ni NPs | 4.58% | 1.55% |

^{1,2} Calculated based on the current intensities at $E = 0.6$ V and $E = 0.7$ V, respectively.

3.5. Quantitative Analysis of Real Samples

3.5.1. Calibration Curve

Voltammetric responses of the CuO/Cu electrode towards increasing concentrations of glucose and glycine have been shown in Figure 4. As can be seen, the oxidation peaks corresponding to glucose and glycine increase with their increasing concentrations, and also shift to higher potentials. Nevertheless, the calibration curves relating the current intensity at the peak maximum with the theoretical COD values (calculated according to $I (\mu\text{A}) = m \cdot c (\text{mg/L O}_2) + b$) were built, showing a linear behavior as shown in Figure 8. The analytical parameters derived from these are summarized in Table 4, where the closeness to 1.0 of the correlation of determination (R^2) confirms the good linearity within the specified range of concentrations. The limit of detection was calculated using the 3σ IUPAC criterion.

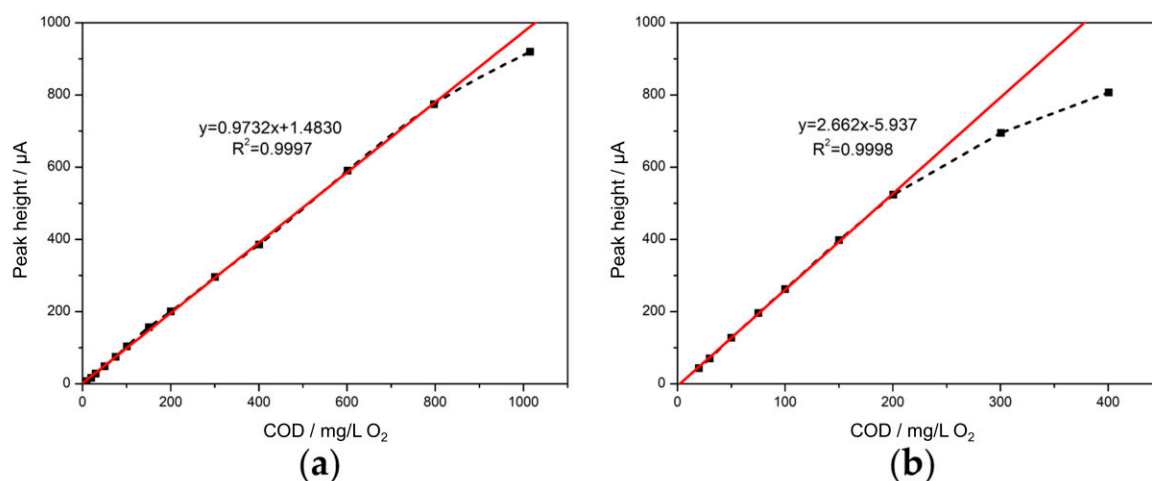


Figure 8. Calibration curves (black dotted curve) obtained from the peak heights of the voltammetric responses of the CuO/Cu electrodes (shown in Figures 4a and 5a) to increasing (a) glucose and (b) glycine. Red lines display the fitted least squares fittings to the linear zone.

Table 4. Calibration lines of the CuO/Cu electrode based on measurement to glucose or glycine, from currents at oxidation peak maxima.

| Compound | Sensitivity ($\mu\text{A}/\text{mg/L O}_2$) | Intercept (μA) | R^2 | Linear Range (mg/L O_2) | Limit of Detection (mg/L O_2) |
|----------|---|-----------------------------|--------|------------------------------------|--|
| Glucose | 0.9732 | 1.48 | 0.9997 | 20–800 | 13.6 |
| Glycine | 2.662 | 5.94 | 0.9998 | 20–200 | 4.1 |

Despite the best behavior in terms of sensitivity was obtained for the CuO/Cu electrode, a good behavior was also obtained for the other ones (calibrations not shown). Another remarkable detail, observable from the graphs in Figures 4 and 5, is the cross-response between the different electrodes, not only from the different potential associated to the various oxidation peaks, but also from the different sensitivities obtained for each of the electrodes and compounds. Overall, this is a situation highly desirable when developing ETs.

3.5.2. Artificial Neural Network Method

Upon completing the characterization of the sensors, the next step was building the actual model that will allow the estimation of COD values in real samples. The aim is that the use of an artificial intelligence response model will allow a better estimation as it combines the responses from different sensors and compensates the differences in the voltammetric responses towards different compounds (e.g., peak position, sensitivity, etc.).

In the interest of proving our hypothesis, glucose and glycine were used as standards. Next, with the conditions described in Section 2.5, the samples consisting of binary mixtures of glucose and glycine were prepared and analyzed employing the sensor array. As evidenced from Figure 6, upon mixing the two organic compounds, there are no longer two separate peaks, but a broader peak is obtained instead. However, different sensitivity is obtained for each compound, thus not being as straightforward the interpolation into a the previous simple univariate calibration curve. For this reason, ANNs were chosen as the tool to build the multivariate calibration model.

After a trial-and-error process in which the topology of the ANN was optimized, the final model had 91 neurons in the input layer (corresponding to the selected points of the voltammograms from the five sensors), seven neurons and *logsig* transfer function in the hidden layer, and one neuron and *purelin* transfer function in the output layer. During the ANN optimization, the inputs were pruned by means of CI analysis, while the number of

neurons and transfer functions were systematically varied to identify the configuration that led to the best performance employing only the data of the training subset. Next, the samples of the test subset were interpolated into the model and the comparison graphs of predicted vs. expected COD were built (Figure 9). As can be seen, a satisfactory performance was obtained for both subsets, with regression lines close to the ideal identity ones. With the aim of numerically quantifying the performance, the regression parameters (as well as the confidence intervals for them) and the root mean square error (RMSE) of the fitting were calculated (Table 5). From the observed values, a good trend is confirmed, as the ideal values of slope and intercept were within the confidence intervals 1 and 0, respectively; furthermore, the coefficient of determination was close to 1 and the RMSE value was relatively low.

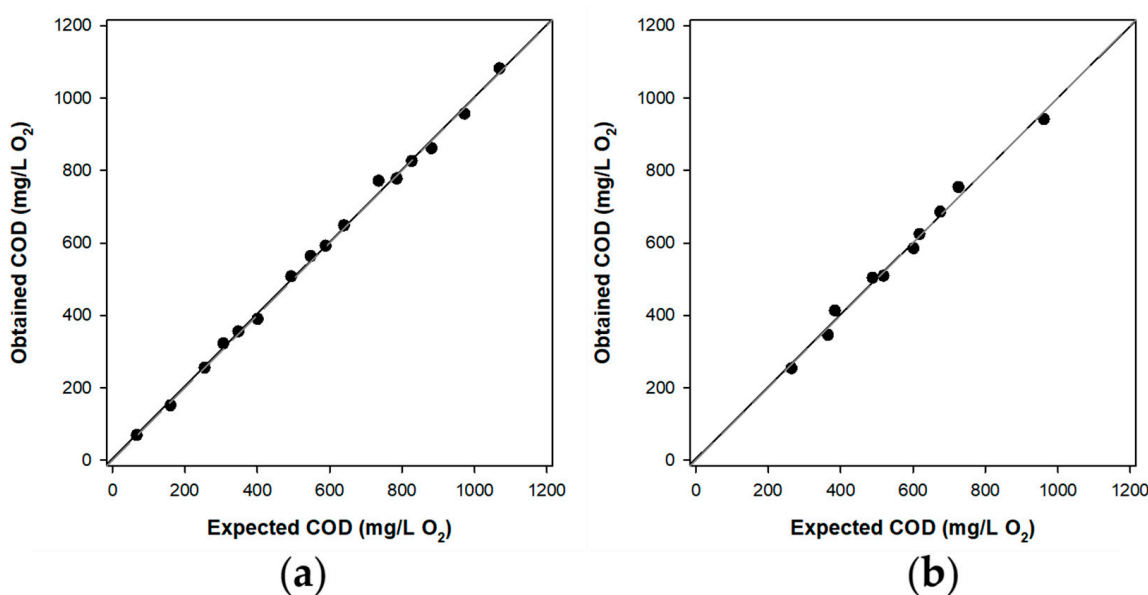


Figure 9. Modeling ability of the optimized CI-ANN for the estimation of COD value. Comparison graphs of predicted vs. expected for the (a) training and (b) testing subsets. The dashed line corresponds to the ideal comparison line ($y = x$).

Table 5. Fitted regression lines for the comparison between obtained vs. expected values for the train and test subsets.

| Data Set | Slope | Intercept (mg/L O ₂) | R ² | RMSE (mg/L O ₂) |
|----------|---------------|----------------------------------|----------------|-----------------------------|
| Training | 0.997 ± 0.027 | 6 ± 18 | 0.998 | 11.3 |
| Testing | 0.996 ± 0.077 | 4 ± 45 | 0.991 | 16.6 |

Finally, upon construction and validation of the model with the standard samples, the last step was its application to the analysis of real samples. The analysis of the real samples didn't require any pre-treatment apart from the dilution 1:1 in the measuring media as we need to preserve the same experimental conditions as in the calibration. In this manner, a total of 10 samples were analyzed, five (samples R1~R5) of them corresponding to the above described in Section 2.5, plus those with spiked concentrations of glucose and glycine (samples S1~S5).

After interpolating responses into the model, the predicted COD values were compared with those obtained employing the reference method, and with the direct interpolation, in this case using the CuO/Cu electrode alone (Table 6). From those values, two remarks have to be made. On the one side, it can be seen how the COD values for the real samples are close to the LODs of the individual sensors, and consequently out of the range of the model. On the other side, it should be taken into account that the various

spiked samples correspond to the different real samples considered, thus meaning that the good behavior is obtained even when different samples are being considered.

Table 6. Results obtained for the real and spiked samples using different methods for estimating the COD values.

| Sample | Spiked COD (mg/L O ₂) | $y = 0.9732x + 1.4830$ ^a COD (mg/L O ₂) | $y = 2.662x - 5.937$ ^b COD (mg/L O ₂) | ANN COD (mg/L O ₂) | Colorimetric COD (mg/L O ₂) |
|--------|-----------------------------------|---|---|-----------------------------------|--|
| R1 | – | 99.32 | 41.88 | – | 12.10 |
| R2 | – | 102.7 | 43.12 | – | 15.10 |
| R3 | – | 98.06 | 41.43 | – | 9.21 |
| R4 | – | 100.8 | 42.43 | – | 5.24 |
| R5 | – | 105.6 | 44.18 | – | 11.70 |
| S1 | 187.3 (glycine) | 481.8 | 178.9 | 141.9 | 216.0 |
| S2 | 376.5 (glucose) | 402.1 | 149.8 | 284.7 | 416.0 |
| S3 | 320.0 (glucose + glycine) | 361.1 | 134.8 | 286.7 | 342.0 |
| S4 | 234.4 (glucose + glycine) | 466.7 | 173.4 | 211.0 | 260.0 |
| S5 | 686.5 (glucose + glycine) | 868.3 | 320.2 | 659.7 | 719.0 |

^a equation corresponding to the calibration of the Cu/CuO disk electrode at the first oxidation peak; ^b equation corresponding to the calibration of the Cu/CuO disk electrode at the second oxidation peak.

With the aim of evaluating which method displayed better agreement with what, an exploratory analysis of the different methodologies was done, in which a comparison of the results from paired samples was performed between the two methodologies, and the regression line calculated. In order to avoid bias in the lowest COD values, results below the LOD were discarded. These results are summarized in the Table 7. In light of these, there are a few observations to be made. First, it is noteworthy how the standard interpolation with the voltammetric data is not capable of obtaining correct results, with limited linearities, and errors in defect. Second, the spiked concentrations could be reasonably predicted, both with the colorimetric reference method (as was expected), but also with the ET method. Third, the best linearity found throughout the comparison, also remarkably close to the identity line, was the one of the colorimetric results vs. those of the ET methodology. This best comparison line is shown in Figure 10, and as can be seen, a good agreement was again obtained between both values, confirming the suitability of the approach.

Table 7. Exploratory analysis of the COD results (mg/L O₂) obtained for the spiked samples with the different methodologies being compared.

| Results Compared | Comparison Line | R ² (n = 5) |
|--------------------------------------|------------------------------|------------------------|
| ET vs. Spiked | $Y = 1.0132 \times X - 48.9$ | 0.9383 |
| Colorimetric vs. Spiked | $Y = 1.0134 \times X + 24.8$ | 0.9553 |
| Volt 1 ^a vs. Spiked | $Y = 0.8532 \times X + 208$ | 0.5384 |
| Volt 2 ^b vs. Spiked | $Y = 0.8701 \times X + 240$ | 0.7413 |
| ET vs. Colorimetric | $Y = 0.9949 \times X - 71.9$ | 0.9723 ^c |
| Volt 1 ^a vs. Colorimetric | $Y = 0.3119 \times X + 78.8$ | 0.5385 |
| Volt 2 ^b vs. Colorimetric | $Y = 0.3181 \times X + 90.7$ | 0.7414 |

^a Current intensity corresponding to the first oxidation peak. ^b Current intensities corresponding to the second oxidation peak. ^c Best determination coefficient.

Lastly, although it is true that other ET systems have already been reported for the estimation of COD values in water [35], one of the key advantages of the approach proposed herein is that the calibration is carried out using standard solutions of model compounds instead of requiring the analysis of some samples previously analyzed with a reference method. Moreover, despite the comparison not being straightforward given disparities in the nature of the considered samples and chemometric tools, a better correlation between the estimated and actual values seems to be obtained in our case than in previous

systems [36–40]. This can be attributed to the nature of the sensors used here. Previous approaches relied on chemo-sensors that were based on bare metallic electrodes, whereas sensors modified with different NPs have been considered herein, with the well-known advantages of NPs in sensors. In addition, some previous approaches relied on the use of enzymatic biosensors, and while it is true that these might typically show a better performance, the presence of contaminants in wastewater can also have a harmful effect on them. This was already stated by Czolkos et al., who reported that when only COD needs to be estimated, the use of a single carbon electrode can yield similar results than an array of enzyme-coated electrodes, obviously a much simpler and cheaper option [39].

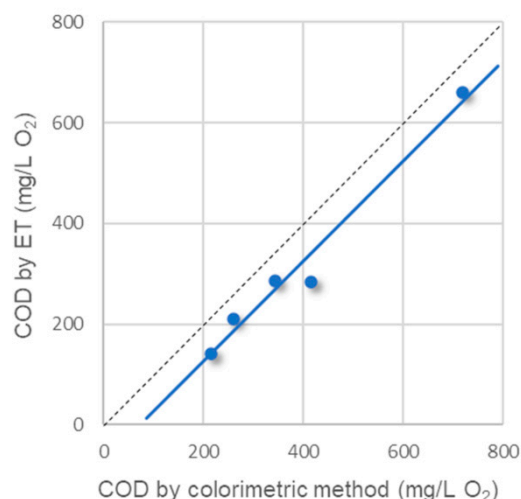


Figure 10. Comparison of results obtained for the spiked real samples, between the proposed ET approach and the reference colorimetric method.

4. Conclusions

In this work, one surface modified Cu/CuO disk electrode and four metal nanoparticle-modified graphite electrodes were fabricated to be employed in the research for the analysis of quantitative organic load. Glucose and glycine were chosen to be standard substances representative of organic contaminants. Based on the electrochemical voltammetric responses of these electrodes, a one-sensor calibration curve method was built, and two calibration curves were obtained from peak heights of voltammetric responses to glucose and glycine, respectively, which showed good correlations in their linear range of each one-analyte system. However, the application of both calibration curves in the practical detection was limited because of the multi-peak responses in multi-analyte samples. Nevertheless, an artificial intelligence response model allows a better estimation by combining the responses from different sensors and compensating the differences in the voltammetric responses to different compounds. Therefore, a five-sensor ET array employed with an ANN model was built. Finally, both methods were applied to real freshwater samples for analysis and prediction. By comparing results detected from those with a reference colorimetric method, the proposed ET model showed a much better performance than the single-sensor calibration curve method.

With this research, we have demonstrated a high value application with neural networks as useful tools to solve a difficult problem in the water and wastewater field [41], here in relation to the prediction of pollution from sensor data.

Author Contributions: Conceptualization, M.d.V.; methodology, M.d.V.; software, X.C.; investigation, Q.W.; writing—original draft preparation, Q.W. and X.C.; writing—review and editing, M.d.V.; funding acquisition, M.d.V. All authors have read and agreed to the published version of the manuscript.

Funding: This research was funded by the Spanish Ministry of Science and Innovation, MCINN (Madrid), grant number PID2019-107102RB-C21/AEI/10.13039/5001100011033. Q.W. acknowledges the concession of a PhD grant of the Chinese Scholarship Council (China).

Institutional Review Board Statement: Not applicable.

Informed Consent Statement: Not applicable.

Data Availability Statement: Not applicable.

Acknowledgments: We acknowledge the help provided by Diana Losantos Velasco, from the Department of Chemical, Biological and Environmental Engineering, Universitat Autònoma de Barcelona, in the colorimetric determination of COD of the real samples.

Conflicts of Interest: The authors declare no conflict of interest.

References

1. Alves, N.A.; Olean-Oliveira, A.; Cardoso, C.X.; Teixeira, M.F.S. Photochemiresistor sensor development based on a bismuth vanadate type semiconductor for determination of chemical oxygen demand. *ACS Appl. Mater. Interfaces* **2020**, *12*, 18723–18729. [[CrossRef](#)] [[PubMed](#)]
2. Hao, N.; Dai, Z.; Xiong, M.; Han, X.; Zuo, Y.; Qian, J.; Wang, K. Rapid potentiometric detection of chemical oxygen demand using a portable self-powered sensor chip. *Anal. Chem.* **2021**, *93*, 8393–8398. [[CrossRef](#)] [[PubMed](#)]
3. Ramon, R.; Valero, F.; del Valle, M. Rapid determination of chemical oxygen demand using a focused microwave heating system featuring temperature control. *Anal. Chim. Acta* **2003**, *491*, 99–109. [[CrossRef](#)]
4. Huang, X.; Zhu, Y.; Yang, W.; Jiang, A.; Jin, X.; Zhang, Y.; Yan, L.; Zhang, G.; Liu, Z. A self-supported CuO/Cu nanowire electrode as highly efficient sensor for COD measurement. *Molecules* **2019**, *24*, 3132. [[CrossRef](#)]
5. Gutiérrez-Capitán, M.; Baldi, A.; Gómez, R.; García, V.; Jiménez-Jorquera, C.; Fernández-Sánchez, C. Electrochemical nanocomposite-derived sensor for the analysis of chemical oxygen demand in urban wastewaters. *Anal. Chem.* **2015**, *87*, 2152–2160. [[CrossRef](#)]
6. Sawyer, C.N.; McCarty, P.L.; Parkin, G.F. *Chemistry for Environmental Engineering and Science*, 5th ed.; McGraw-Hill Education: New York, NY, USA, 2002; pp. 625–626.
7. Yu, H.; Ma, C.; Quan, X.; Chen, S.; Zhao, H. Flow injection analysis of chemical oxygen demand (COD) by using a boron-doped diamond (BDD) electrode. *Environ. Sci. Technol.* **2009**, *43*, 1935–1939. [[CrossRef](#)]
8. Diksy, Y.; Rahmawati, I.; Jiwanti, P.K.; Ivandini, T.A. Nano-Cu modified Cu and nano-Cu modified graphite electrodes for chemical oxygen demand sensors. *Anal. Sci.* **2020**, *36*, 1323–1330. [[CrossRef](#)]
9. Zhou, Y.; Jing, T.; Hao, Q.; Zhou, Y.; Mei, S. A sensitive and environmentally friendly method for determination of chemical oxygen demand using NiCu alloy electrode. *Electrochim. Acta.* **2012**, *74*, 165–170. [[CrossRef](#)]
10. Zhang, Z.; Chang, X.; Chen, A. Determination of chemical oxygen demand based on photoelectrocatalysis of nanoporous TiO₂ electrodes. *Sens. Actuators B Chem.* **2016**, *223*, 664–670. [[CrossRef](#)]
11. Jin, W.; Maduraiveeran, G. Electrochemical detection of chemical pollutants based on gold nanomaterials. *Trends Environ. Anal. Chem.* **2017**, *14*, 28–36. [[CrossRef](#)]
12. Orozco, J.; Fernández-Sánchez, C.; Mendoza, E.; Baeza, M.; Céspedes, F.; Jiménez-Jorquera, C. Composite planar electrode for sensing electrochemical oxygen demand. *Anal. Chim. Acta* **2008**, *607*, 176–182. [[CrossRef](#)] [[PubMed](#)]
13. Cheng, Q.; Wu, C.; Chen, J.; Zhou, Y.; Wu, K. Electrochemical tuning the activity of nickel nanoparticle and application in sensitive detection of chemical oxygen demand. *J. Phys. Chem. C* **2011**, *115*, 22845–22850. [[CrossRef](#)]
14. Wang, Q.; del Valle, M. Determination of chemical oxygen demand (COD) using nanoparticle-modified voltammetric sensors and electronic tongue principles. *Chemosensors* **2021**, *9*, 46. [[CrossRef](#)]
15. Duan, W.; Gunes, M.; Baldi, A.; Gich, M.; Fernández-Sánchez, C. Compact fluidic electrochemical sensor platform for on-line monitoring of chemical oxygen demand in urban wastewater. *Chem. Eng. J.* **2022**, *449*, 137837. [[CrossRef](#)]
16. Hou, Y.; Hu, J.; Liu, L.; Zhang, J.; Cao, C. Effect of calcination temperature on electrocatalytic activities of Ti/IrO₂ electrodes in methanol aqueous solutions. *Electrochim. Acta* **2006**, *51*, 6258–6267. [[CrossRef](#)]
17. Wang, J.Q.; Wu, C.; Wu, K.B.; Cheng, Q.; Zhou, Y.K. Electrochemical sensing chemical oxygen demand based on the catalytic activity of cobalt oxide film. *Anal. Chim. Acta* **2012**, *736*, 55–61. [[CrossRef](#)]
18. Ai, S.; Gao, M.; Yang, Y.; Li, J.; Jin, L. Electrocatalytic sensor for the determination of chemical oxygen demand using a lead dioxide modified electrode. *Electroanalysis* **2004**, *16*, 404–409. [[CrossRef](#)]
19. Li, J.; Li, L.; Zheng, L.; Xian, Y.; Jin, L. Rh₂O₃/Ti electrode preparation using laser anneal and its application to the determination of chemical oxygen demand. *Meas. Sci. Technol.* **2006**, *17*, 1995–2000. [[CrossRef](#)]
20. Ma, C.; Tan, F.; Zhao, H.; Chen, S.; Quan, X. Sensitive amperometric determination of chemical oxygen demand using Ti/Sb-SnO₂/PbO₂ composite electrode. *Sens. Actuators B Chem.* **2011**, *155*, 114–119. [[CrossRef](#)]
21. Silva, C.R.; Conceição, C.D.C.; Bonifácio, V.G.; Fatibello Filho, O.; Teixeira, M.F.S. Determination of the chemical oxygen demand (COD) using a copper electrode: A clean alternative method. *J. Solid State Electrochem.* **2009**, *13*, 665–669. [[CrossRef](#)]
22. Carchi, T.; Lapo, B.; Alvarado, J.; Montero, P.J.E.; Llorca, J.; Fernández, L. A nafion film cover to enhance the analytical performance of the CuO/Cu electrochemical sensor for determination of chemical oxygen demand. *Sensors* **2019**, *19*, 669. [[CrossRef](#)] [[PubMed](#)]
23. Hassan, H.H.; Badr, I.H.A.; Abdel-Fatah, H.T.M.; Elfeky, E.M.S.; Abdel-Aziz, A.M. Low cost chemical oxygen demand sensor based on electrodeposited nano-copper film. *Arab. J. Chem.* **2018**, *11*, 171–180. [[CrossRef](#)]

24. Hanrahan, G. Computational neural networks driving complex analytical problem solving. *Anal. Chem.* **2010**, *82*, 4307–4313. [[CrossRef](#)]
25. Liu, J.; Xu, Y.; Liu, S.; Yu, S.; Yu, Z.; Low, S.S. Application and progress of chemometrics in voltammetric biosensing. *Biosensors* **2022**, *12*, 494. [[CrossRef](#)] [[PubMed](#)]
26. Aroca-Santos, R.; Cancilla, J.C.; Matute, G.; Torrecilla, J.S. Identifying and quantifying adulterants in extra virgin olive oil of the picual varietal by absorption spectroscopy and nonlinear modeling. *J. Agric. Food Chem.* **2015**, *63*, 5646–5652. [[CrossRef](#)]
27. Gutiérrez, A.; Calvo, D.; Céspedes, F.; del Valle, M. Automatic sequential injection analysis electronic tongue with integrated reference electrode for the determination of ascorbic acid, uric acid and paracetamol. *Microchim. Acta* **2007**, *157*, 1–6. [[CrossRef](#)]
28. Cetó, X.; Gonzalez-Calabuig, A.; Capdevila, J.; Puig-Pujol, A.; del Valle, M. Instrumental measurement of wine sensory descriptors using a voltammetric electronic tongue. *Sens. Actuators B Chem.* **2015**, *207*, 1053–1059. [[CrossRef](#)]
29. González-Calabuig, A.; del Valle, M. Voltammetric electronic tongue to identify Brett character in wines. On-site quantification of its ethylphenol metabolites. *Talanta* **2018**, *179*, 70–74. [[CrossRef](#)]
30. Serrano, N.; González-Calabuig, A.; del Valle, M. Crown ether-modified electrodes for the simultaneous stripping voltammetric determination of Cd(II), Pb(II) and Cu(II). *Talanta* **2015**, *138*, 130–137. [[CrossRef](#)]
31. del Valle, M. Sensor arrays and electronic tongue systems. *Int. J. Electrochem.* **2012**, *2012*, 986025. [[CrossRef](#)]
32. Cetó, X.; Céspedes, F.; del Valle, M. Comparison of methods for the processing of voltammetric electronic tongues data. *Microchim. Acta* **2013**, *180*, 319–330. [[CrossRef](#)]
33. Dhara, K.; Mahapatra, D.R. Electrochemical nonenzymatic sensing of glucose using advanced nanomaterials. *Microchim. Acta* **2018**, *185*, 49.
34. American Public Health Association; American Water Works Association; Water Environment Federation. *Standard Methods for the Examination of Water and Wastewater*, 23rd ed.; American Public Health Association: Washington, DC, USA; American Water Works Association: Washington, DC, USA; Water Environment Federation: Washington, DC, USA, 2017.
35. Cetó, X.; del Valle, M. Electronic tongue applications for wastewater and soil analysis. *iScience* **2022**, *25*, 104304. [[CrossRef](#)] [[PubMed](#)]
36. Tønning, E.; Sapelnikova, S.; Christensen, J.; Carlsson, C.; Winther-Nielsen, M.; Dock, E.; Solna, R.; Skladal, P.; Nørgaard, L.; Ruzgas, T.; et al. Chemometric exploration of an amperometric biosensor array for fast determination of wastewater quality. *Biosens. Bioelectron.* **2005**, *21*, 608–617. [[CrossRef](#)]
37. Gutiérrez, A.; Céspedes, F.; del Valle, M.; Louthander, D.; Krantz-Rülcker, C.; Winquist, F. A flow injection voltammetric electronic tongue applied to paper mill industrial waters. *Sens. Actuators B Chem.* **2006**, *115*, 390–395. [[CrossRef](#)]
38. Campos, I.; Alcañiz, M.; Aguado, D.; Barat, R.; Ferrer, J.; Gil, L.; Marrakchi, M.; Martínez-Mañez, R.; Soto, J.; Vivancos, J.-L. A voltammetric electronic tongue as tool for water quality monitoring in wastewater treatment plants. *Water Res.* **2012**, *46*, 2605–2614. [[CrossRef](#)]
39. Czolkos, I.; Dock, E.; Tønning, E.; Christensen, J.; Winther-Nielsen, M.; Carlsson, C.; Mojzík, R.; Skladal, P.; Wollenberger, U.; Nørgaard, L.; et al. Prediction of wastewater quality using amperometric bioelectronic tongues. *Biosens. Bioelectron.* **2016**, *75*, 375–382. [[CrossRef](#)]
40. Legin, E.; Zadorozhnaya, O.; Khaydukova, M.; Kirsanov, D.; Rybakin, V.; Zagrebina, A.; Ignatyeva, N.; Ashina, J.; Sarkar, S.; Mukherjee, S.; et al. Rapid evaluation of integral quality and safety of surface and waste waters by a multisensor system (electronic tongue). *Sensors* **2019**, *19*, 2019. [[CrossRef](#)]
41. Bui, H.M.; Bui, H.N.; Le, T.M.; Karri, R.R. Application of artificial neural networks on water and wastewater prediction: A review. In *Soft Computing Techniques in Solid Waste and Wastewater Management*; Karri, R.R., Ravindran, G., Dehghani, M.H., Eds.; Elsevier: Amsterdam, The Netherlands, 2021; pp. 95–109.